Design of Multi-Plet Perfect Reconstruction Filter Banks Using Frequency-Response Masking Technique

K. M. Tsui, S. C. Chan, *Member, IEEE*, and Yong Ching Lim, *Fellow, IEEE*

***Abstract*—This paper proposes a new design method for a class of two-channel perfect reconstruction (PR) filter banks (FBs) called multi-plet FBs with very sharp cutoff using frequency-response masking (FRM) technique. The multi-plet FBs are PR FBs and their frequency characteristics are controlled by a single subfilter. By recognizing the close relationship between the subfilter and the FRM-based halfband filter, very sharp cutoff PR multi-plet FBs can be realized with reduced implementation complexity. The design procedure is very general and it can be applied to both linear-phase and low-delay PR FBs. Design examples are given to demonstrate the usefulness of the proposed method.**

***Index Terms*—Frequency-response masking, lifting structure, low-delay, multi-plet, perfect reconstruction filter banks.**

I. Introduction

PERFECT reconstruction (PR) filter banks (FBs) have important applications in digital signal processing and communications. Due to the nonlinear PR conditions, designing general PR FBs is considered to be a difficult problem, especially for FBs with tight frequency specifications such as sharp cutoff, high stopband attenuation and large number of channels. Therefore, FBs that structurally satisfies the PR conditions have received considerable attention recently. An efficient structure of two-channel biorthogonal FIR/IIR FBs, which satisfies this property, is the structural PR FB proposed in [1]. In a related PR FB called triplet FB [2]–[4], a generalization of the structure in [1], more design freedom is available and it is possible to achieve a more symmetric frequency response. More recently, the structural PR FBs [1] and the triplet FBs [2]–[4], which respectively involve two and three lifting steps [5], are extended to so-called multi-plet FBs with multiple lifting steps [6], [7]. Moreover, the concept of frequency transformation of digital filters previously studied in [8] can be applied directly to the lifting structure to obtain another PR FB with same number of lifting steps and similar frequency characteristics but a narrower transition bandwidth. The multi-plet FBs can also be viewed as an extension of the work in [9] for frequency transformation of PR FBs.

Recently, frequency-response masking (FRM) technique has been shown to be an efficient method for reducing the arithmetic complexity of implementing digital filters with very sharp cutoff [10]. Subsequently, it has also been applied to the realization of single-rate fast filter banks [11], [12]. Although there is considerable interest in employing FRM technique to design nearly PR cosine-modulated FBs (transmultiplexers) [13], the possibility of constructing multirate PR FBs using FRM technique is still an open problem.

In this paper, we study the design of sharp cutoff multi-plet PR FBs using FRM technique. However, directly synthesizing the subfilter in the multi-plet FBs using FRM technique may not be so effective because the subfilter, which controls the frequency characteristics of the multi-plet FBs, has a constant magnitude response except that it drops to zero at $\omega = \pi$. Since it does not contain a well-defined stopband, there is little freedom in designing the masking filters in the FRM structure. Fortunately, it is shown that, with appropriate scaling, the subfilter is indeed one of the polyphase components of a halfband filter (HBF) (the one which is not a pure delay term). Consequently, by using the results of FRM-based HBFs previously proposed in [14] and [15], very sharp cutoff subfilters and hence multi-plet PR FBs with low arithmetic complexity can be obtained. The concept is similar to the work in [16] and [17], which were concerned with the synthesis of linear-phase FIR Hilbert transformers using FRM technique.

In [7], it was also shown that multi-plet FBs with reduced delay can be obtained by employing low-delay FIR/IIR subfilters instead of linear-phase FIR subfilters. Motivated by this result, we further propose to extend the linear-phase FIR FRM-based HBFs to the low-delay case so that approximately passband linear-phase FIR FRM-based subfilter with lower group delay can be obtained. To further reduce the arithmetic complexity, multi-level FRM-based subfilters is also studied. Design results show that the proposed approach offers significantly lower arithmetic complexity than conventional multi-plet FBs at the expense of slight increase in system delay. The proposed FRM-based multi-plet FBs are attractive in high-speed multirate applications requiring high frequency selectivity where arithmetic complexity is of an important concern. For instance, the proposed FBs can be applied to the frequency excisers, which are used to suppress narrowband interference in direct-sequence spread spectrum (DSSS) systems [18]–[21]. Usually, the performance of frequency excisers will improve with higher fre-

Manuscript received April 24, 2007; revised October 18, 2007. First published March 07, 2008; current version published October 29, 2008. This paper was recommended by Associate Editor S.-M. Phoong.

K. M. Tsui and S. C. Chan are with the Department of Electrical and Electronic Engineering, The University of Hong Kong, Pokfulam, Hong Kong (e-mail: kmtsui@eee.hku.hk, scchan@eee.hku.hk).

Y. C. Lim is with the School of Electrical and Electronics Engineering, Nanyang Technological University, Singapore 639798 (e-mail: elelimyc@pmail.ntu.edu.sg).

Digital Object Identifier 10.1109/TCSI.2008.920086

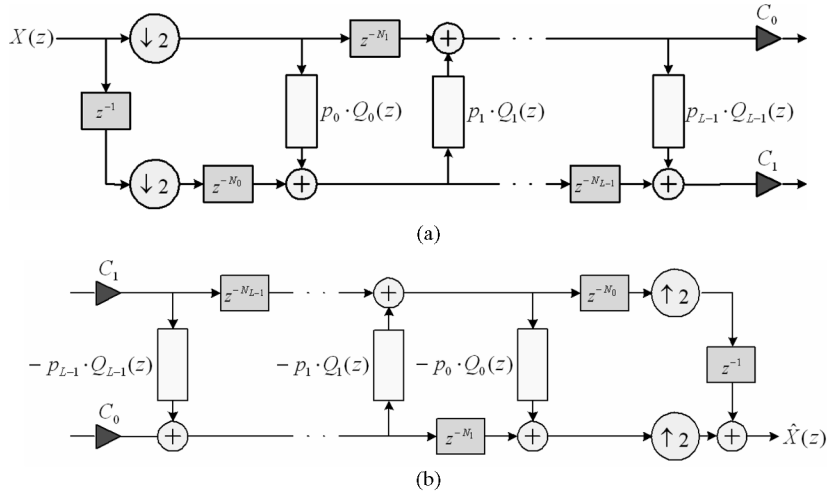

Fig. 1. Structure of the multi-plet FBs: (a) Analysis bank. (b) Synthesis bank.

quency selectivity because of the reduction of interband spectral leakage. The paper is organized as follows. The principle of the multi-plet FBs is briefly reviewed in Section II. Their relations to the FRM-based HBFs and problem formulation of the proposed FRM-based subfilters are discussed respectively in Sections III and IV. Finally, the conclusion is presented in Section V.

II. Multi-Plet Two-Channel Structural PR FBS

The general structure of the multi-plet two-channel FBs is shown in Fig. 1. It is parameterized by L subfilters $Q_m(z)$, L delay parameters N_m, L lifting coefficients p_m, and two scaling constants C_0 and C_1 for $m = 0, 1, \ldots, L-1$. It can be seen from Fig. 1 that the z-transforms of the analysis and synthesis filters in the lifting structure are given by

$$\begin{aligned} H_0(z) &= C_0 H^{(L-2)}(z), \quad H_1(z) = C_1 H^{(L-1)}(z), \\ F_0(z) &= H_1(-z) \text{ and } F_1(z) = -H_0(-z), \\ \text{where } H^{(0)}(z) &= z^{-2N_0-1} + p_0 \cdot Q_0(z^2), \\ H^{(1)}(z) &= z^{-2N_1} + p_1 \cdot Q_1(z^2) H^{(0)}(z) \text{ and} \\ H^{(m)}(z) &= z^{-2N_m} H^{(m-2)}(z) + p_m \\ &\quad \cdot Q_m(z^2) H^{(m-1)}(z) \end{aligned} \tag{2-1}$$

for $m = 2, 3, \ldots, L-1$. We shall consider a special case of lifting where the subfilters are identical:

$$Q_{L-1}(z^2) = \cdots = Q_1(z^2) = Q_0(z^2) = Q(z^2). \tag{2-2}$$

Note that for a certain scaling $H_0(z)$ is a halfband filter (HBF) with one of the polyphase components equal to a signal delay and the other equal to the subfilter $Q(z)$. For causal implementation, the delay parameters N_m should be

$$N_{L-1} = \cdots = N_2 = N_1 = G \text{ and } N_0 = \frac{(G-1)}{2} \tag{2-3}$$

where G is the passband group delay of $Q(z^2)$. As a result, the group delays of the analysis filter pair, $H_0(z)$ and $H_1(z)$, are respectively given by

$$G_0 = (L-1) \cdot G \text{ and } G_1 = L \cdot G. \tag{2-4}$$

When the identical subfilter has the form of $(1+z^{-1})/2$, the resulting FB is referred to as the prototype lifting structured FB. This prototype FB can be transformed to a new FB with narrower transition bandwidth using the following substitution of variable:

$$\widetilde{x} = R_Q(x) = z^G Q(z^2) \tag{2-5}$$

where $\widetilde{x} = (\widetilde{z} + \widetilde{z}^{-1})/2$ and $R_Q(x)$ is the zero-phase response of $Q(z^2)$ for some positive integer G. To avoid possible confusion, all the symbols associated with the prototype FB before transformation are augmented by the symbol "$\sim$". For instance, the z-transform variable z and its associated variable x as mentioned in (2-5) for the prototype FB are now denoted by $\widetilde{z}$ and $\widetilde{x}$, respectively. For filters and FBs after transformation, and other common parameters such as N_m, p_m, C_0 and C_1, the conventional notations without the symbol "$\sim$" will be employed. Similarly, the digital frequencies before and after transformation are related by $\widetilde{x} = \cos(\widetilde{\omega}) = R_Q(x) = R_Q(\cos(\omega))$, where ω and $\widetilde{\omega}$ are respectively the digital radian frequencies of the prototype and transformed FBs. Since the transformed FB is obtained by using the substitution in (2-5), it can also be implemented by the same number of lifting steps as the prototype filter. Fig. 2 illustrates the effect of the transformation and shows the relations of the prototype FB, the subfilter and the transformed multi-plet FB. Interested readers are referred to [7] for more details.

As a result, if the subfilter $Q(z)$, which is one of the polyphase components of the HBF, can be implemented using FRM technique, then very sharp cutoff multi-plet FBs with low arithmetic complexity can be realized. Details will be discussed in Section III.

III. Frequency-Response Masking Based Subfilter

A. Relations Between Subfilter and Halfband Filter

From the discussion in Section II, the ideal zero-phase response of the subfilter $Q(z)$ can be summarized as follows:

$$\begin{cases} \cos(\widetilde{\omega}_c) \le R_Q(\widehat{x}) \le 1, & 0 \le \omega \le \omega_c \\ -1 \le R_Q(\widehat{x}) \le -\cos(\widetilde{\omega}_c), & \pi - \omega_c \le \omega_r \omega \le \pi \end{cases} \tag{3-1}$$

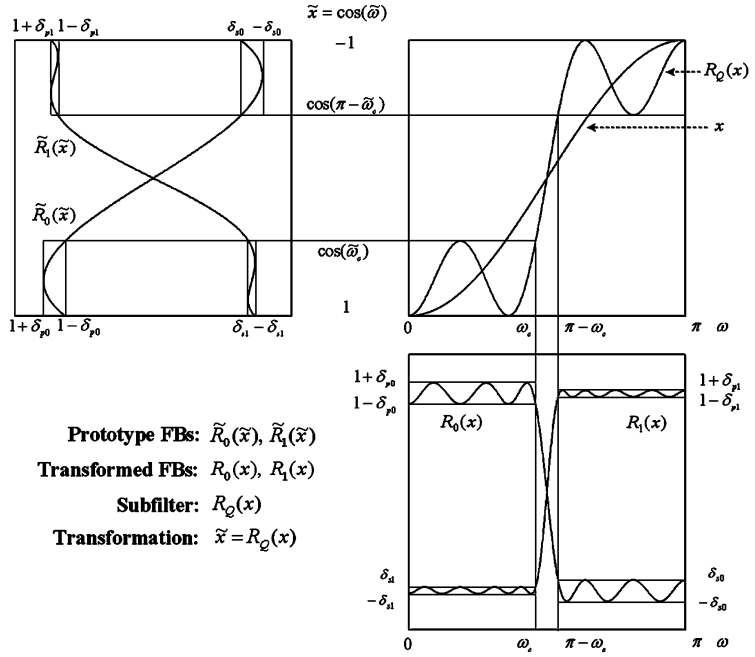

Fig. 2. General relations and specifications of the prototype FB, the subfilter and the transformed multi-plet FB.

where $\widetilde{\omega}_c$ and ω_c are respectively the passband cutoff frequencies of the prototype and the transformed FBs as shown in the top left and bottom right figures of Fig. 2. Alternatively, by introducing a delay term $e^{-j\omega G}$ into (3-1), the desired causal response of the subfilter can be rewritten as

$$Q_d(\omega) = \begin{cases} m \cdot e^{-j\omega G/2}, & 0 \le \omega \le 2\omega_c \\ 0 & \omega = \pi \end{cases} \tag{3-2}$$

with the maximum allowable error

$$\delta_Q = \frac{[1 - \cos(\widetilde{\omega}_c)]}{2} \tag{3-3}$$

where $m = [1 + \cos(\widetilde{\omega}_c)]/2$. Therefore, the subfilter $Q(z)$ can be realized as an even-length linear-phase FIR filter with a symmetric impulse response satisfying the specification in (3-1). In this case, it is observed that $Q(z)$ is related to a linear-phase FIR HBF $B(z)$ as

$$B(z) = 0.5[m^{-1}Q(z^2) + z^{-G}] \tag{3-4}$$

with identical passband and stopband ripples. To satisfy the given specifications in (3-2) and (3-3), we have

$$\omega_{c,B} = \omega_c \text{ and } \delta_B = \frac{\delta_Q}{2} \tag{3-5}$$

where $\omega_{c,B}$ and δ_B are respectively the passband cutoff frequency and the maximum design error of $B(z)$. Therefore, the Kaiser's formula [22] can be used to estimate the length of $B(z)$ (L_B) as follows:

$$L_B \approx \frac{-20\log_{10}\left(\frac{\delta_Q}{2}\right) - 13}{2.324 \cdot (\pi - 2\omega_c)} + 1. \tag{3-6}$$

Hence, we have

$$L_Q \approx \frac{(L_B + 3)}{2} \tag{3-7}$$

where L_Q is the length of $Q(z)$.

B. Realization of Subfilter Using FRM Technique

In the general FRM technique [10], a digital filter can be expressed as

$$B(z) = C(z^M)D(z) + [z^{-M\tau_C} - C(z^M)]\hat{D}(z) \tag{3-8}$$

where $C(z)$ is called the model filter with a group delay of τ_C samples, $D(z)$ and $\hat{D}(z)$ are called the masking filters, and M is an integer. Since the subfilter can be derived from an HBF, it is interesting to examine the structure of a FRM-based HBF. More precisely, if $B(z)$ is the FRM-based HBF, then we have [14], [15]

$$C(z) = C_0(z^2) + 0.5z^{-\tau_C} \tag{3-9a}$$
$$\hat{D}(z) = z^{-\tau_D} - (-1)^{\tau_D}D(-z) \tag{3-9b}$$
$$M \text{ is an odd positive integer} \tag{3-9c}$$

where τ_D is the group delay of $D(z)$. Since an HBF in general has odd sample delay, τ_C and τ_D are respectively odd and even positive integers. Let $D(z) = D_0(z^2) + z^{-1}D_1(z^2)$ be the polyphase decomposition of $D(z)$, then (3-9b) can be rewritten as $\hat{D}(z) = z^{-\tau_D} - D_0(z^2) + z^{-1}D_1(z^2)$. Using this result and substituting (3-9) into (3-8), we can express $B(z)$ as the following polyphase representation:

$$\begin{aligned} B(z) &= B_0(z^2) + z^{-1}B_1(z^2) \\ B_0(z) &= C_0(z^M)[2D_0(z) - z^{-\tau_D/2}] + z^{-(M\tau_C+1)/2}D_1(z) \\ B_1(z) &= 0.5 \cdot z^{-(M\tau_C+\tau_D-1)/2}. \end{aligned} \tag{3-10}$$

Comparing (3-4) and (3-10), one finds the desired FRM-based subfilter as follows:

$$Q(z) = 2mB_0(z). \tag{3-11}$$

The corresponding structure is shown in Fig. 3.

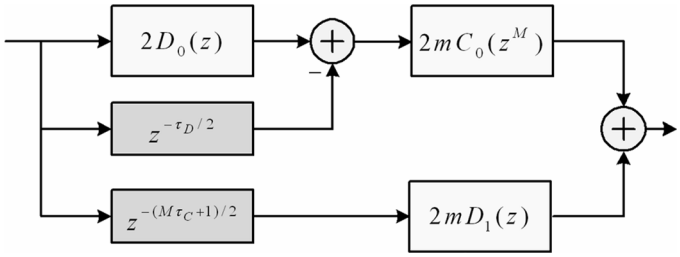

Fig. 3. Structure of FRM-based subfilter.

C. Selection of Filters' Lengths and M

Given the value of M, there are two possible cases for $C(z)$ and $D(z)$ to satisfy the specifications of $B(z)$ in (3-5) [14], [15]. In case 1, we have

$$\begin{aligned} M &= 4k+1, \\ \omega_{c,C} &= M\omega_{c,B} - 2k\pi, \\ M\omega_{p,D} &= 2k\pi + \omega_{c,C}, \\ M\omega_{s,D} &= (2k+1)\pi + \omega_{c,C} \text{ and} \\ \delta_C &= \delta_D = \delta_B \end{aligned} \tag{3-12}$$

whereas in case 2, we have

$$\begin{aligned} M &= 4k-1, \\ \omega_{c,C} &= M\omega_{c,B} + (2k-M)\pi, \\ M\omega_{p,D} &= (2k-1)\pi - \omega_{c,C}, \\ M\omega_{s,D} &= 2k\pi - \omega_{c,C} \text{ and} \\ \delta_C &= \delta_D = \delta_B \end{aligned} \tag{3-13}$$

where k is a positive integer; $\omega_{c,C}$ is the passband cutoff frequency of $C(z)$; $\omega_{p,D}$ and $\omega_{s,D}$ are respectively the passband and stopband cutoff frequencies of $D(z)$; δ_C and δ_D are respectively the maximum allowable errors of $C(z)$ and $D(z)$. Using these results, the filter lengths of $C(z)$ and $D(z)$ can again be estimated respectively using the Kaiser's formula as follows:

$$L_C \approx \frac{f(\delta_Q)}{M(\pi - 2\omega_c)} + 1 \text{ and } L_D \approx \frac{Mf(\delta_Q)}{\pi} + 1 \tag{3-14}$$

where $f(\delta_Q) = [-20\log_{10}(\delta_Q/2) - 13]/2.324$. Therefore, the total number of nonzero coefficients of $C(z)$ and $D(z)$ is approximately given by

$$T(M) \approx \frac{f(\delta_Q)}{2M(\pi - 2\omega_c)} + \frac{Mf(\delta_Q)}{\pi}. \tag{3-15}$$

Since $T(M)$ is a convex function for $M > 0$, the optimal value of M can be determined by setting the derivative of $T(M)$ to zero and it gives

$$M_{opt} \approx \sqrt{\frac{\pi}{2(\pi - 2\omega_c)}}. \tag{3-16}$$

Note that M should be chosen as the odd nearest integer to M_{opt} for practical implementation. Similar derivation can be found in [17], where the lengths of $D_0(z)$ and $D_1(z)$ in (3-10) are considered separately.

IV. Problem Formulation

It was shown in [7] that the transformation method in Section II also works well for approximately passband linear-phase subfilters. More precisely, $\widetilde{x}$ in (2-5) is now transformed to $R_Q(x)$, which is a complex quantity. This is similar to the low-delay triplet PR FB in [4], where the subfilters are chosen as low-delay (approximately passband linear-phase), instead of linear-phase, FIR filters. The advantage over their linear-phase counterparts is that the overall system delay of the transformed FBs can be reduced. As seem from (3-10), the passband group delay of the FRM-based $B(z)$ is given by $M\tau_C + \tau_D$. To further reduce the group delay of the FRM-based subfilter, it is desirable to design model filter $C(z)$ and masking filter $D(z)$ with low passband group delay. In this paper, we propose to separately design $C(z)$ and $D(z)$ in turn using second order cone programming (SOCP) [23] so that it is not necessary to determine the "don't care" bands of $D(z)$ due to the images of stopband of $C(z^M)$. An advantage of using SOCP is that the formulations of designing $C(z)$ and $D(z)$ provided below are applicable to both linear-phase and low-delay cases. Alternatively, one may also employ the method in [24] to simultaneously design $C(z)$ and $D(z)$, which requires iterative optimization. Note that for the same specifications, designing $C(z)$ and $D(z)$ simultaneously should in principle offer better performance than designing them separately. However, if the problem is very complex as in the case of multi-level FRM technique (to be discussed in Section V), it may not be easy to arrive at the global minimum when all filters are designed simultaneously. On the other hand, the proposed approach has advantages of simplicity, reliability and good performance because each individual problem is just a simple and convex FIR filter design problem.

A. Design of Model Filter $C(z)$

Consider the frequency response of the HBF $C(z)$

$$C(e^{j\omega}) = 0.5e^{-j\omega\tau_C} + C_0(e^{j2\omega}) \tag{4-1}$$

where $C_0(e^{j\omega}) = \sum_{n=0}^{(L_C-1)/2} c_0(n)e^{-j\omega n}$, τ_C and L_C are chosen to be odd positive integers. On the other hand, the HBF is a lowpass filter and its desired frequency response can be written as

$$C_d(\omega) = \begin{cases} e^{-j\omega\tau_C} & 0 < \omega < \omega_{c,C} \\ 0 & \pi - \omega_{c,C} < \omega < \pi. \end{cases} \tag{4-2}$$

Note that τ_C may be less than $(L_C - 1)/2$ so that low-delay HBFs can be obtained. Instead of directly approximating $C_d(\omega)$, we shall consider the following equivalent problem in the minimax sense:

$$\min_{c_0(n)} \max_{\omega} \left| C_0(e^{j\omega}) - C_{0,d}(\omega) \right|, \quad \omega \in [0, 2\omega_{c,C}] \tag{4-3}$$

where $C_{0,d}(\omega)$ is the desired response of $C_0(e^{j\omega})$, which is given by

$$C_{0,d}(\omega) = \begin{cases} e^{-j\omega\tau_C/2}, & 0 \le \omega \le 2\omega_{c,C} \\ 0, & \omega = \pi. \end{cases} \tag{4-4}$$

To formulate the minimization problem in (4-3) as a SOCP problem, $C_0(e^{j\omega})$ is first expressed in terms of the design variables $\boldsymbol{c}_0 = [c_0(0), \ldots, c_0((L_C-1)/2)]^T$ as

$$C_0(e^{j\omega}) = \boldsymbol{c}_0^T \boldsymbol{e}_C(\omega) \tag{4-5}$$

where $[\boldsymbol{c}_0]_k = c_0(k)$ and $[\boldsymbol{e}_C(\omega)]_k = e^{-j\omega k}$, for $k = 0, \ldots, (L_C-1)/2$; $[\bullet]_k$ denotes the kth entry of the column vector inside the square bracket. Hence, (4-3) can be rewritten as

$$\begin{aligned} \min_{\boldsymbol{c}_0} \quad & \delta \\ \text{s. t.} \quad & \delta - [\alpha_R^2(\omega) + \alpha_I^2(\omega)]^{1/2} \geq 0 \\ & \omega \in [0, 2\omega_{c,C}] \boldsymbol{c}_0^T \boldsymbol{e}_C(\pi) = 0 \end{aligned} \tag{4-6}$$

where δ is an auxiliary variable, $\alpha_R(\omega) = \mathrm{Re}\left[\boldsymbol{c}_0^T \boldsymbol{e}_C(\omega) - C_{0,d}(\omega)\right]$, $\alpha_I(\omega) = \mathrm{Im}\left[\boldsymbol{c}_0^T \boldsymbol{e}_C(\omega) - C_{0,d}(\omega)\right]$, and $\mathrm{Re}[\bullet]$ and $\mathrm{Im}[\bullet]$ denote respectively the real and imaginary parts of the elements inside the square bracket. Discretizing the frequency variable ω over a dense set of frequencies $\{\omega_i, i = 1, \ldots, K_\omega\}$ in the frequency of interest, the inequality constraints in (4-6) becomes $\delta - [\alpha_R^2(\omega_i) + \alpha_I^2(\omega_i)]^{1/2} \geq 0$ for $i = 1, \ldots, K_\omega$. Finally, by defining the augmented variable $\boldsymbol{y}_C = [\delta \quad \boldsymbol{c}_0^T]^T$, (4-6) can be cast to the following standard SOCP problem:

$$\begin{aligned} \min_{\boldsymbol{y}_C} \quad & \boldsymbol{\theta}_C^T \boldsymbol{y}_C \\ \text{s. t.} \quad & \boldsymbol{\theta}_C^T \boldsymbol{y}_C \geq \|\boldsymbol{U}_C(\omega_i)\boldsymbol{y}_C - \boldsymbol{v}_C(\omega_i)\|_2 \quad i = 1, \ldots, K_\omega \\ & \boldsymbol{g}^T \boldsymbol{y}_C = 0 \end{aligned} \tag{4-7}$$

where $\boldsymbol{\theta}_C = [1 \quad \boldsymbol{O}_{(L_C+1)/2}^T]^T$; $\boldsymbol{U}_C(\omega_i) = \begin{bmatrix} 0 & \mathrm{Re}[\boldsymbol{e}_C(\omega_i)]^T \\ 0 & \mathrm{Im}[\boldsymbol{e}_C(\omega_i)]^T \end{bmatrix}$; and $\boldsymbol{v}_C(\omega_i) = \begin{bmatrix} \mathrm{Re}[C_{0,d}(\omega_i)] \\ \mathrm{Im}[C_{0,d}(\omega_i)] \end{bmatrix}$; $\boldsymbol{g} = [0 \quad \boldsymbol{e}_C(\pi)^T]^T$; $\|\cdot\|_2$ denotes the Euclidean norm; and $\boldsymbol{O}_N$ is a $N \times 1$ zero vector.

B. Design of Masking Filter $D(z)$

Suppose that the frequency response of D_z is given by

$$D(e^{j\omega}) = \sum_{n=0}^{L_D-1} d(n) e^{-j\omega n} \tag{4-8}$$

the impulse response $d(n)$ can be determined similarly by approximating the desired response of $D(z)$ (i.e., $e^{-j\omega\tau_D}$ in the passband and zero in the stopband; τ_D is even). However, one should have to know the locations of the "don't care" bands due to the images of stopband of $C(z^M)$ in order to reduce the implementation complexity of $D(z)$ [10]. Instead, we propose to solve the following minimization problem directly:

$$\min_{d(n)} \max_{\omega} \left| B(e^{j\omega}) - B_d(\omega) \right|, \quad \omega \in \Omega_B \tag{4-9}$$

where $B(e^{j\omega})$ can be expressed in terms of $D(e^{j\omega})$ given $C_0(e^{j\omega})$, $B_d(\omega)$ is the desired frequency response of $B(e^{j\omega})$ in the frequency of interest Ω_B like the one in (4-2) with the subscript C replaced with B. As such, the desired specification of $D(z)$ can be simplified, because the "don't care" bands are handled automatically. More precisely, the minimization problem in (4-9) can be reformulated as

$$\min_{\boldsymbol{d}} \delta \text{ s.t. } \delta - \left[\beta_R^2(\omega) + \beta_I^2(\omega)\right]^{1/2} \geq 0, \quad \omega \in \Omega_B \tag{4-10}$$

where $\beta_R(\omega) = \mathrm{Re}[\boldsymbol{d}^T \boldsymbol{\phi}(\omega) - \Psi(\omega)]$, $\beta_I(\omega) = \mathrm{Im}[\boldsymbol{d}^T \boldsymbol{\phi}(\omega) - \Psi(\omega)]$, $[\boldsymbol{d}]_k = d(k)$, $\boldsymbol{\phi}(\omega) = \boldsymbol{e}_D(\omega)[e^{-j\omega M\tau_C} + C_0(e^{j\omega 2M})] - \boldsymbol{e}_D(\omega + \pi)[e^{-j\omega M\tau_C} - C_0(e^{j\omega 2M})]$, $[\boldsymbol{e}_D(\omega)]_k = e^{-j\omega k}$, $k = 0, \ldots, L_D - 1$, and $\Psi(\omega) = e^{-j\omega\tau_D}\left[e^{-j\omega M\tau_C} - C_0(e^{j\omega 2M})\right] + B_d(\omega)$. After discretizing the frequency variable ω, (4-10) can be written as the following SOCP problem

$$\begin{aligned} \min_{\boldsymbol{y}_D} \quad & \theta_D^T \boldsymbol{y}_D \\ \text{s.t.} \quad & \theta_D^T \boldsymbol{y}_D \geq \|\boldsymbol{U}_D(\omega_i)\boldsymbol{y}_D - \boldsymbol{v}_D(\omega_i)\|_2, \\ & i = 1, \ldots, K_\omega \end{aligned} \tag{4-11}$$

where $\boldsymbol{\theta}_D = [1 \quad \boldsymbol{O}_{L_D}^T]^T$; $\boldsymbol{U}_D(\omega_i) = \begin{bmatrix} 0 & \mathrm{Re}[\boldsymbol{\phi}(\omega_i)]^T \\ 0 & \mathrm{Im}[\boldsymbol{\phi}(\omega_i)]^T \end{bmatrix}$; and $\boldsymbol{v}_D(\omega_i) = \begin{bmatrix} \mathrm{Re}[\Psi(\omega_i)] \\ \mathrm{Im}[\Psi(\omega_i)] \end{bmatrix}$.

TABLE I
LIFTING COEFFICIENTS AND SCALING CONSTANTS OF THE PR PROTOTYPE FBS

	Triplet FB [3], [4]	Optimized FB
p_0	$1-\sqrt{2}$	0.23987556667257
p_1	$1/\sqrt{2}$	-0.54571527976115
p_2	$1-\sqrt{2}$	0.54045911345798
p_3	N/A	-0.23167459250035
C_0	$1/\sqrt{2}$	0.71237102180672
C_1	$1/\sqrt{2}$	0.71401331291255

C. Example: Two-Channel PR FBs

In this example and the subsequent one in Section V, the frequency variable ω in the band of interest was uniformly discretized into $K_\omega = 500$ evenly spaced samples. The SOCP optimization was carried out using the *SeDuMi* Matlab Toolbox [25] and it took less than a few seconds to obtain the solution on a Pentium4 3.2 GHz personal computer.

As an illustration, the prototype FB used in the triplet FB [3], [4] is considered. The corresponding lifting coefficients and scaling constants are listed in the second column of Table I and the frequency response is shown in Fig. 4(a). The target specifications are: 0.015 dB passband deviation, -30 dB stopband attenuation and $\omega_c = 0.49\pi$. From Fig. 4(a), $\tilde{\omega}_c$ should be chosen as 0.08π (and hence $\delta_Q \approx 0.0157$) so as to satisfy the prescribed passband and stopband ripples. In order for a linear-phase FIR subfilter to satisfy (3-1), its filter length L_Q is chosen to be 104 according to (3-7). The frequency response of the transformed FB using linear-phase FIR subfilter is shown in Fig. 4(b).

For purpose of comparison, a linear-phase FIR FRM-based subfilter is also designed. To satisfy the given specifications mentioned previously, the passband cutoff frequency and the maximum ripple error of the FRM-based HBF $B(z)$ are respectively chosen as 0.49π and 0.00785. The upsampling factor M and the lengths of $C(z)$ and $D(z)$ are determined to be 5, 43, and

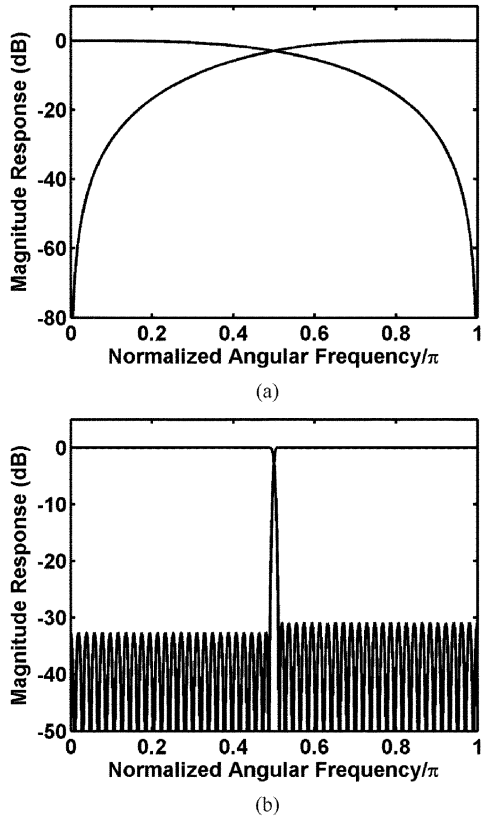

Fig. 4. Frequency responses of (a) prototype FB used in triplet FB [3], [4] and (b) multi-plet FB using linear-phase FIR subfilter.

21, respectively. Note that the linear-phase FIR FRM-based subfilter has slightly higher group delay, but considerably lower implementation complexity than its conventional counterpart designed above. Fig. 5(a) shows the frequency response of the corresponding multi-plet FB.

To reduce the system delay, the model filter is chosen as a low-delay FIR HBF with a group delay of $\tau_C = 13$ samples. The corresponding frequency response is shown in Fig. 5(b). The overall group delay of the FRM-based subfilter is now reduced from 57.5 samples to 37.5 samples. Therefore, the system delays of the analysis lowpass and highpass filters becomes respectively 150 and 225 samples, as compared with 230 and 345 samples in the linear-phase case. It can also be seen from Fig. 5(c) that the low-delay multi-plet FB is approximately linear-phase in the passband with peak group delay errors of 0.48 samples for $H_0(z)$, and 0.35 samples for $H_1(z)$. Table II summarizes the design parameters and results of the example.

It should be noted that the arithmetic complexity of the low-delay subfilters can further be reduced by employing FRM-based allpass filters [15] and IIR filters [26]. Moreover, it is possible to construct wavelet bases by imposing K-regularity conditions to FRM-based multi-plet FBs. These conditions are indeed equivalent to imposing flatness constraints to the subfilter under the SOCP framework. However, details are omitted due to page limitation. Interested readers are referred to [7] for more details.

V. Multi-Level FRM-Based Subfilter

For extremely narrow transition bandwidth, it is possible to decompose $C_0(z)$ in (3-10) to further reduce the implementation complexity [17]. More precisely, (3-10) can be generalized to

$$C_0^{(r-1)}(z) = C_0^{(r)}(z^{M^{(r)}}) \cdot \left[2D_0^{(r)}(z) - z^{-\tau_D^{(r)}/2}\right] + z^{-\left(M^{(r)}\tau_C^{(r)}+1\right)/2} \cdot D_1^{(r)}(z), \quad \text{for } r = 1, \ldots, R \tag{5-1}$$

where the superscript (r) implies the rth level of FRM structure, $C_0^{(0)}(z) = B_0(z)$ and R is the number of decomposition. Given the specifications of $C^{(r-1)}(z)$, the specifications of $C^{(r)}(z)$ and $D^{(r)}(z)$ can be determined using (3-12) or (3-13). Similar to the discussion in Section III, the total number of nonzero

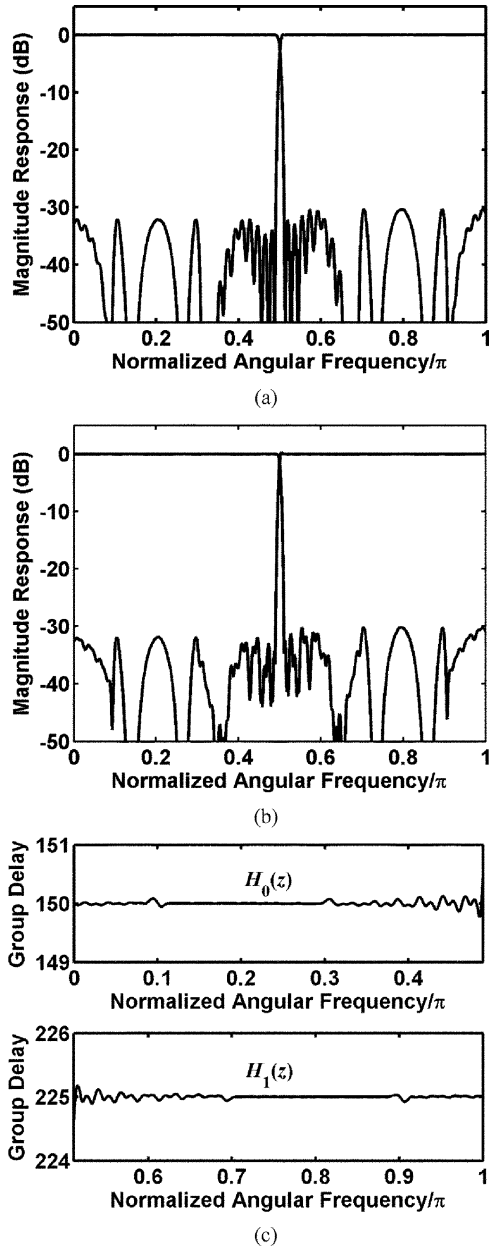

Fig. 5. (a) Frequency response of multi-plet FB using linear-phase FRM-based subfilter. (b) Frequency and (c) group delay responses of multi-plet FB using low-delay FRM-based subfilter.

TABLE II
SUMMARY OF THE DESIGN EXAMPLE

	LP FIR	LP FIR FRM	LD FIR FRM
L_Q (τ_Q)	104 (51.5)	116* (57.5)	116* (37.5)
L_C (τ_C)	N/A	43 (21)	43 (13)
L_D (τ_D)	N/A	21 (10)	21 (10)
τ_{H0}, τ_{H1}	206, 309	230, 345	150, 225
δ_{g0}, δ_{g1}	0, 0	0, 0	0.48, 0.35

τ_{Hi}: Group delay of $H_i(z)$.
δ_{gi}: Passband group delay error of $H_i(z)$, $i = 0, 1$.
LP: Linear phase.
LD: Low delay.
* Effective length of FRM-based subfilter.

coefficients can be approximated as

$$T(M^{(1)},\ldots,M^{(R)}) \approx \frac{f(\delta_Q)}{2(\pi-2\omega_c)\prod_{r=1}^{R} M^{(r)}} + \frac{f(\delta_Q)}{\pi}\sum_{r=1}^{R} M^{(r)} \quad (5\text{-}2)$$

and the optimal value of $M^{(r)}$ is given by

$$M_{opt}^{(r)} \approx \left[\frac{\pi}{2(\pi-2\omega_c)}\right]^{1/(R+1)}, \quad r = 1,\ldots,R. \quad (5\text{-}3)$$

From (5-1), a R-level FRM-based subfilter composes of $R+1$ filters, namely $C_0^{(R)}(z)$ and $D^{(r)}(z)$ for $r = 1,\ldots,R$. Here, we propose to design the target filter $C_0^{(0)}(z)$ starting from $C_0^{(R)}(z)$ followed by $D^{(r)}(z)$, $r = R,\ldots,1$, so that the design approach mentioned in Section IV can be similarly extended to this case. For instance when $R = 2$, $C_0^{(2)}(z)$ and $D^{(2)}(z)$ are first designed. Then $C_0^{(1)}(z)$ is constructed using (5-1), and finally $D^{(1)}(z)$ is designed given $C_0^{(1)}(z)$.

A. Example: 8-Channel PR FB

In this example, we shall consider the design of a multi-channel uniform FB using the tree structure and the proposed FRM-based multi-plet FB. Fig. 6 shows a two-stage tree-structured analysis filter bank. One advantage of using tree-structured FBs is that it avoids nonlinear constrained optimizations with large number of variables. In addition, the PR condition is structurally imposed to the final multi-channel FB if the component two-channel FBs are PR FBs. Therefore, the tree-structured FB serves as an attractive alternative for designing uniform PR FBs with very large number of channels. In this case, the savings of arithmetic complexity using FRM technique would be more pronounced owing to less spacing between consecutive channels. To obtain a regular transition bandwidth $\Delta\omega$ in each channel, the transition bandwidth of the two-channel FB at each stage should satisfy the following conditions [27]:

$$\Delta\omega_j = 2^{j-1}\Delta\omega \quad (5\text{-}4)$$

where $\Delta\omega_j$ is the transition bandwidth of the analysis filter pair at the jth stage. As the transition bandwidth increases with the stage of the tree structure, the arithmetic complexity of the component two-channel FBs decreases as the stage increases. Therefore, FRM or multi-level FRM techniques are expected to be very useful to the implementation of the component FBs at the initial stages of the tree-structured FB. The overall increase in system delay is also reasonable as their downsampling factors are much smaller than those at the final stages.

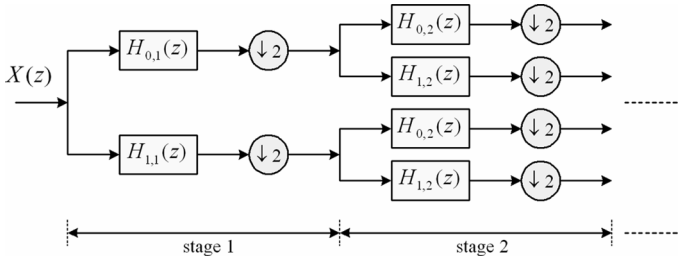

Fig. 6. Two-stage tree-structured analysis FB.

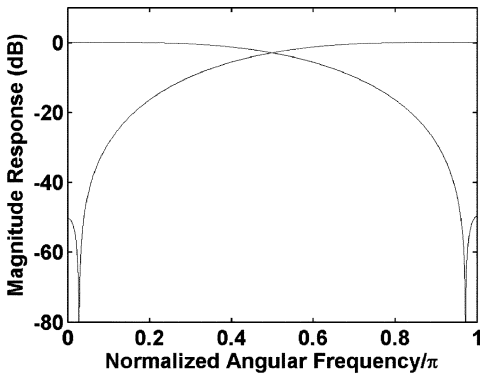

Fig. 7. Frequency responses of prototype FB with symmetric response.

For illustrative purpose, an 8-channel uniform FB is designed by cascading three stages of two-channel multi-plet FBs. The target passband derivation and stopband attenuation are 5×10^{-4} dB and -50 dB, respectively. The target transition bandwidth is 0.01π and therefore the required cutoff frequencies for the three stages are respectively 0.01π, 0.02π and 0.04π. As discussed in [7], different combinations of prototype FBs and subfilters can be employed to satisfy the given specification. Fig. 7 shows another prototype FB, which is obtained from example 1 in [7]. Table I summarizes the corresponding lifting coefficients and scaling constants. The multi-plet FBs in the first and second stages are realized using two-level FRM technique with $M^{(1)} = M^{(2)} = 3$, whereas the last one is realized using one-level FRM technique with $M^{(1)} = 3$. The specifications and parameters of the subfilters at all stages are summarized in Table III. Note that the number of levels and parameters are chosen such that the lowest implementation complexity is achieved at the expense of increased delay. Also, other design options exist to satisfy the same specifications. The frequency responses of the analysis filter pairs at the three stages and the resulting 8-channel FB are shown in Fig. 8. The total number of nonzero coefficients of the resulting 8-channel FB is 344, which is about 45% of that designed without employing FRM technique. Note that due to the narrow transition band of the first analysis filter pair, more stages can be cascaded to realize

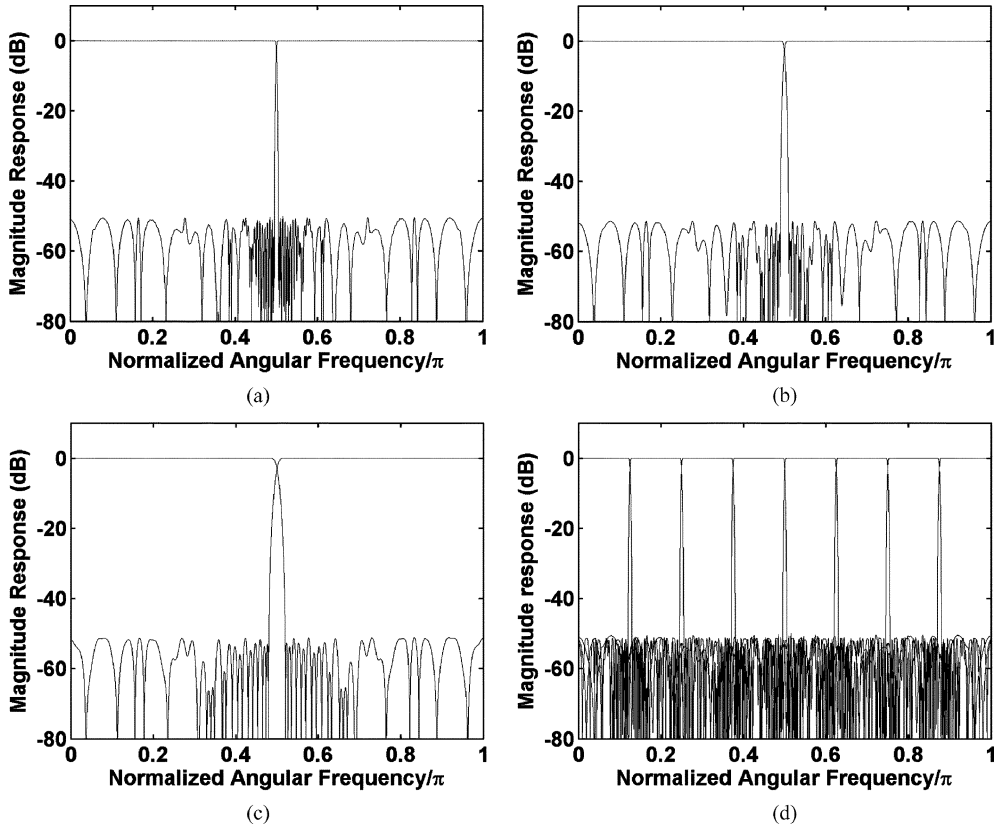

Fig. 8. Design results of the 8-channel FRM-based FB. (a), (b), and (c) Frequency responses of the analysis filter pair at stages 1, 2, and 3, respectively. (d) Frequency response of the 8-channel FB.

TABLE III
DESIGN PARAMETERS OF FRM-BASED SUBFILTERS IN THE 8-CHANNEL FB

First Stage		
	LP FIR	LP FIR FRM
$\Delta\omega$	0.01π	
L_Q	248	348*
$L_C^{(2)}$, $L_D^{(2)}$, $L_D^{(1)}$	N/A	71, 17, 17
$M^{(2)}$, $M^{(1)}$	N/A	3, 3
Second Stage		
	LP FIR	LP FIR FRM
$\Delta\omega$	0.02π	
L_Q	124	186*
$L_C^{(2)}$, $L_D^{(2)}$, $L_D^{(1)}$	N/A	35, 17, 17
$M^{(2)}$, $M^{(1)}$	N/A	3, 3
Third Stage		
	LP FIR	LP FIR FRM
$\Delta\omega$	0.04π	
L_Q	64	84*
$L_C^{(1)}$, $L_D^{(1)}$	N/A	51, 17
$M^{(1)}$	N/A	3

∗ Effective length of FRM-based subfilter.

FBs with more number of channels. The above result suggests that the proposed FRM-based approach is very effective in reducing the arithmetic complexity of the sharp cutoff multi-plet FBs. They are attractive in high-speed multirate applications involving high frequency selectivity, such as the frequency excisers in DSSS systems [18]–[21], where arithmetic complexity is an important concern.

VI. CONCLUSION

The design of two-channel multi-plet PR FBs using FRM techniques is presented. By employing the subfilter derived by FRM-based HBF in the lifting structure, very sharp cutoff PR FBs can be realized with low implementation complexity. The use of low-delay FIR FRM-based subfilters is also proposed to further reduce the system delay of the sharp cutoff multi-plet FBs.

REFERENCES

[1] S. M. Phoong, C. W. Kim, P. P. Vaidyanathan, and R. Ansari, "A new class of two-channel biothogonal filter banks and wavelet bases," *IEEE Trans. Signal Process.*, vol. 43, pp. 649–664, Mar. 1995.
[2] R. Ansari, C. W. Kim, and M. Dedovic, "Structure and design of two-channel filter banks derived from a triplet of halfband filters," *IEEE Trans. Circuits Syst. II*, vol. 46, pp. 1487–1496, 1999.
[3] D. B. H. Tay, "A novel approach to the design of the class of triplet halfband filterbanks," *IEEE Trans. Circuits Syst. II*, vol. 57, no. 7, pp. 378–383, Jul. 2004.
[4] S. C. Chan and K. S. Yeung, "On the design and multiplier-less realization of perfect reconstruction triplet-based FIR filter banks and wavelet bases," *IEEE Trans. Circuits Syst. I*, vol. 51, no. 8, pp. 1476–1491, Aug. 2004.
[5] I. Daubechies and W. Sweldens, "Factoring wavelet transform into lifting steps," *J. Fourier Anal. Appl.*, vol. 4, no. 3, pp. 247–269, 1998.

[6] S. C. Chan and K. M. Tsui, "Multi-plet two-channel perfect reconstruction filter banks," in *Proc. IEEE ISCAS'2005*, May 23–26, 2005, pp. 4297–4300.
[7] K. M. Tsui and S. C. Chan, "Multi-plet two-channel FIR and causal stable IIR perfect reconstruction filter banks," *IEEE Trans. Circuits Syst. I*, vol. 53, no. 12, pp. 2804–2817, Dec. 2006.
[8] T. Saramäki, "Design of FIR filters as a tapped cascaded interconnection of identical subfilters," *IEEE Trans. Circuits Syst*, vol. 34, no. 9, pp. 1011–1029, Sep. 1987.
[9] D. B. H. Tay and N. G. Kingsbury, "Flexible design of multidimensional perfect reconstruction FIR 2-band filters using transformations of variables," *IEEE Trans. Image Process.*, vol. 2, pp. 466–480, Oct. 1993.
[10] Y. C. Lim, "Frequency-response masking approach for the synthesis of sharp linear phase digital filters," *IEEE Trans. Circuits Syst.*, vol. CAS-33, pp. 357–364, Apr. 1986.
[11] L. Yong and W. Ying, "A computationally efficient nonuniform FIR digital filter bank for hearing aids," *IEEE Trans. Circuits Syst. I*, vol. 52, no. 12, pp. 2754–2762, Dec. 2005.
[12] J. W. Lee and Y. C. Lim, "Efficient implementation of real filter banks using frequency-response masking techniques," in *Proc. IEEE APCCAS'2002*, Oct. 28–31, 2002, vol. 1, pp. 69–72.
[13] M. B. Furtado, Jr, P. S. R. Diniz, S. L. Netto, and T. Saramäki, "On the design of high-complexity cosine-modulated transmultiplexers based on the frequency-response masking approach," *IEEE Trans. Circuits Syst. I*, vol. 52, no. 11, pp. 2413–2426, Nov. 2005.
[14] T. Saramäki, Y. C. Lim, and R. Yang, "The synthesis of half-band filter using frequency-response masking technique," *IEEE Trans. Circuits Syst. II*, vol. 42, no. 1, pp. 58–60, Jan. 1995.
[15] H. Johansson and L. Wanhammar, "Filter structures composed of allpass and FIR filters for interpolation and decimation by a factor of two," *IEEE Trans. Circuits Syst II*, vol. 46, pp. 896–905, 1999.
[16] Y. C. Lim and Y. J. Yu, "Synthesis of very sharp Hilbert transformer using the frequency-response masking technique," *IEEE Trans. Signal Process.*, vol. 53, pp. 2595–2597, Jul. 2005.
[17] Y. C. Lim, Y. J. Yu, and T. Saramäki, "Optimum masking levels and coefficient sparseness for Hilbert transformers and half-band filters designed using the frequency-response masking technique," *IEEE Trans. Circuits Syst. I*, vol. 52, no. 11, pp. 2444–2453, Nov. 2005.
[18] M. J. Medley, G. J. Saulnier, and P. K. Das, "Narrow-band interference excision in spread spectrum systems using lapped transforms," *IEEE Trans. Commun.*, vol. 45, no. 11, pp. 1444–1455, Nov. 1997.
[19] M. V. Tazbay and A. N. Akansu, "Adaptive subband transforms in time-frequency excisers for DSSS communications systems," *IEEE Trans. Signal Process.*, vol. 43, pp. 1776–1782, Nov. 1995.
[20] M. J. Medley, G. J. Saulnier, and P. K. Das, "Wavelets and filterbanks in spread spectrum systems," in *Subband and Wavelet Transforms: Design and Applications*, A. N. Akansu and M. J. T. Smith, Eds. Boston, MA: Kluwer, 1995.
[21] A. N. Akansu, M. V. Tazebay, M. J. Medley, and P. K. Das, "Wavelet and subband transforms: fundamentals and communication applications," *IEEE Commun. Mag.*, pp. 104–115, Dec. 1997.
[22] A. V. Oppenheim, R. W. Schafer, and J. R. Buck, *Discrete-Time Signal Processing*. Upper Saddle River, NJ: Prentice-Hall, 1999.
[23] K. M. Tsui, S. C. Chan, and K. S. Yeung, "Design of FIR digital filters with prescribed flatness and peak error constraints using second order cone programming," *IEEE Trans. Circuits Syst. II*, vol. 52, no. 9, pp. 601–605, Sep. 2005.
[24] W. S. Lu and T. Hinamoto, "Optimal design of frequency-response masking filters using second-order cone programming," *IEEE Trans. Circuits Syst. I*, vol. 50, no. 11, pp. 1401–1412, Nov. 2003.
[25] J. F. Sturm, "Using SeDuMi 1.02, a MATLAB toolbox for optimization over symmetric cones," *Optim. Math. Software*, vol. 11–12, pp. 625–653, 1999.
[26] H. H. Chen and S. C. Chan, "A semi-definite programming (SDP) method for designing IIR sharp cut-off digital filters using frequency-response masking," in *Proc. IEEE ISCAS'2004*, May 23–26, 2004, vol. 3, pp. 149–152.
[27] X. M. Xie, S. C. Chan, and T. I. Yuk, "M-band perfect-reconstruction linear-phase filter banks," in *Proc. 11th IEEE Signal Process. Workshop Statist. Signal Process.*, 2001, pp. 583–586.

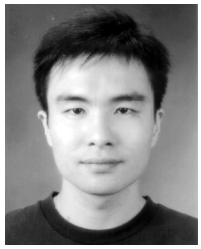

K. M. Tsui received the B.Eng. and M.Phil. degrees in electrical and electronic engineering from The University of Hong Kong in 2001 and 2004, respectively. He is currently working toward the Ph.D. degree in electrical and electronic engineering at the same university.

His main research interests are in biomedical signal processing, digital signal processing, multirate filter bank and wavelet design, and digital filter design, realization and application.

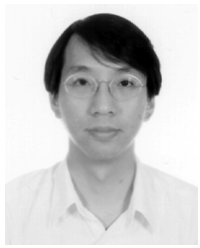

S. C. Chan (S'87–M'92) received the B.Sc. (Eng.) and Ph.D. degrees from the University of Hong Kong in 1986 and 1992, respectively.

He joined City Polytechnic of Hong Kong in 1990 as an Assistant Lecturer and later as a University Lecturer. Since 1994, he has been with the Department of Electrical and Electronic Engineering, The University of Hong Kong, and is now an Associate Professor. He was a visiting researcher in Microsoft Corporation, Redmond, WA, and Microsoft, Beijing, China, at 1998 and 1999, respectively. His research interests include fast transform algorithms, filter design and realization, multirate signal processing, communications signal processing, and image-based rendering.

Dr. Chan is currently a member of the Digital Signal Processing Technical Committee of the IEEE Circuits and Systems Society. He was Chairman of the IEEE Hong Kong Chapter of Signal Processing from 2000 to 2002.

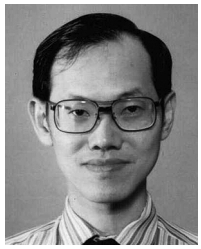

Yong Ching Lim (S'79–M'82–SM'92–F'00) received the A.C.G.I. and B.Sc. degrees in 1977 and the D.I.C. and Ph.D. degrees in 1980, all in electrical engineering, from Imperial College, University of London, London, U.K.

Since 2003, he has been with the School of Electrical and Electronic Engineering, Nanyang Technological University, Singapore, where he is currently a Professor. From 1980 to 1982, he was a National Research Council Research Associate in the Naval Postgraduate School, Monterey, CA. From 1982 to 2003, he was with the Department of Electrical Engineering, National University of Singapore. His research interests include digital signal processing and VLSI circuits and systems design.

Dr. Lim was a recipient of the 1996 IEEE Circuits and Systems Society's Guillemin–Cauer Award, the 1990 IREE (Australia) Norman Hayes Memorial Award, 1977 IEE (U.K.) Prize and the 1974-1977 Siemens Memorial (Imperial College) Award. He served as a Lecturer for the IEEE Circuits and Systems Society under the Distinguished Lecturer Program from 2001 to 2002 and as an associate editor for the IEEE TRANSACTIONS ON CIRCUITS AND SYSTEMS from 1991 to 1993 and from 1999 to 2001. He has also served as an associate editor for *Circuits, Systems and Signal Processing* from 1993 to 2000. He served as the Chairman of the DSP Technical Committee of the IEEE Circuits and Systems Society from 1998 to 2000. He served in the Technical Program Committee's DSP Track as the Chairman in IEEE ISCAS'97 and IEEE ISCAS'00 and as a Co-chairman in IEEE ISCAS'99. He is the General Chairman for IEEE APCCAS 2006 and a General Co-Chair for IEEE ISCAS 2009. He is a member of Eta Kappa Nu.